CHAPTER 2

NUMERICAL ANALYSIS OF STAGGER TUNNED GYRO-TWYSTRON*

*Part of this work has been published as:

S. G. Yadav, Akash and M. Thottappan, "Design and Simulation Investigations of Stagger-Tuned W-Band Gyro-Twystron," in *IEEE Transactions on Electron Devices*, vol. 69, no. 2, pp. 777-784, Feb. 2022, doi:10.1109/TED.2021.3137366.

2.1. Introduction

In Chapter 1, we discussed the history, physics, and classification of microwave tubes up to the gyro-twystron. The CRM mechanism and the operating principle of the different devices based on this principle are discussed in detail and lead us to gyro-twystron review. The detail literature surveys of gyro-twystron are suggested it as an potential applications in millimeter-wave high-resolution radar and high- density, high-directivity communication systems. The gyro-amplifiers required for radar applications must usually be capable of high average power and bandwidth. This urge for wide bandwidth led to exploring various methods to improve the device output performance.

To increase the bandwidth of a gyro-twystron, one can go for stagger tunning [116], where the cavities are tuned with slightly different eigen frequencies. The effect of stagger-tuning on the performance of gyro amplifiers has been reported in the literature by many authors. [117]-[120],[123]. Nusinovich *et al.* [4] have developed the linear and nonlinear theories related to stagger-tuned gyro-twystron and reported a significant increment in bandwidth and gain-bandwidth product as compared to synchronously tuned device [117],[118].

Stagger-tuning increases the bandwidth and simultaneously decreases device gain. To optimize device performance, the gain-bandwidth product trade-off must be examined in detail. Since, gain-bandwidth product is an important parameter for amplifier performance. Thus, this chapter examines how stagger-tuning affects the bandwidth, gain, and gain-bandwidth product of the designed gyro-twystron amplifier.

In the present work, the Various design techniques are imported from the parental gyro-amplifiers of gyro-twystron to design the different sub assemblies [109], [114]. The cavity dimensions are optimized so that the cut-off frequency is less than the operating mode's operating frequency. Similarly, the drift tube radius and length are

chosen to ensure adequate isolation between the two sections. For stable operation, the waveguide length is kept less than the critical length of the backward wave mode. The available generalized theory [116],[118],[118] has been extended for the performance improvement of our designed three-cavity gyro-twystron amplifier. So, the objective of this chapter is:

- Design and optimisation of the different sub-assemblies of present gyro-twystron, as well as its working principal (i.e. dispersion diagram) is discussed in section 2.3.
- Nonlinear analysis is used to study the motion of electron beam in the background of electromagnetic wave supported by the interaction structure and a static axial magnetic field, .
- Here, we have used a technique by which the device gain and bandwidth can be expressed as the dependent on frequency mismatch or stagger tuning thus provides gain and bandwidth variation. Optimize this variable gain and bandwidth term simultaneously, result an optimized gain bandwidth product.

2.2. Design of Sub Sections of Stagger Tuned Gyro-Twystron

There are several factors to take into account when deciding on the design parameters of a three cavity stagger tuned gyro-twystron. The paramount factors are operating mode, operating frequency, suppression of different competing modes, and required outputs that decide the physical dimension of the different sections, i.e., cavity, drift tube, and waveguide. The current design operates in an TE_{01} mode at 94 GHz. Since the azimuthally symmetrical TE_{01} mode has a radial maximum halfway between the wall and the center and there is also a low ohmic power dissipation at high average power operation, these factors led to its selection as the operating mode [125]. With the

consideration of operating mode and operating frequency the design methodology of each sub units is discussed in next section.

2.2.1. Design of Input Cavity Section

The RF input cavity is an essential part of a velocity modulating device because it is where the initial velocity modulation happens. Its primary function is to pre-modulate the electron beam utilizing the electric field developed inside the input cavity by the input RF power. The simplest configuration of the cavity supports oscillations only in the fundamental operating mode. The input cavity is designed to provide the modulated electron beam, whose cutoff frequency remains lower than the desired operating frequency. The cavity radius is defined as, $r_{cav} = x_{mn}c/\omega_c$, where the x_{mn} is the eigenvalue of the operating TE_{mn} mode and ω_c is the angular cut-off frequency of the cavity. The cavity length is kept lower than the drift tube length in order to have sufficient energy for modulation to arise inside the cavity. Simultaneously, it should also be optimized to achieve the desired resonating frequency. The resonating frequency is defined as

$$f_r = \left(c/2\pi\sqrt{\mu_r\varepsilon_r}\right)\left(\sqrt{\left(x_{mn}/r_{cav}\right)^2 + \left(\pi d/l_{cav}\right)^2}\right) \qquad [2.1]$$

where μ_r, ε_r, d and l_{cav} are the relative permittivity, relative permeability, half wave periodicity in axial direction and cavity length. For the stable operation, the beam current must be kept below the start oscillation current (SOL) threshold value, which is proportional to the cavity length [110]. If the current value exceeds that threshold, the modulating cavity starts to oscillate due to noise, just like a gyrotron. To limit this oscillation, the cavities are loaded with the dielectric material to optimize the length and quality factor. The reduction in quality factor is depends on the dimension and dielectric property of the lossy material.

2.2.2. Design of Pre bunching Section or Drift Tube

Isolation between adjacent sections is one of the practical design restrictions that govern the device design. The field free drift tube is designed to provide the desired isolation between adjacent sections. The dimensions of the drift tube are optimized as to provide the effective isolation as well as avoid the beam interception with the drift tube wall. The drift tube radius (r_{dt}) is depends on the following inequalities $r_{dt} < x_{mn}c/2\pi f$ and $r_b < r_{dt} < r_c, r_w$, where r_b and r_w are the gyrating beam radius and waveguide radius. The length of the drift tube is kept enough to provide the sufficient beam bunching and effective isolation between the various cavities and in between the cavity and waveguide. The drift tube length is computed as:

$$L_{dt} = X \Big/ \sqrt{\left(x_{mn}/r_{dt}\right)^2 - \left(\omega/c\right)^2} \qquad [2.2]$$

where ω is the device operating frequency and X is the isolation factor, derived from cold cavity dispersion relation [125].

The eigenvalue of the TE_{11} mode is lower than that of the operating TE_w mode which causes beam interception inside the beam propagation medium. Since, different sections of the device are designed with respect to the TE_{01} mode, the immediate lower TE_{21} mode is chosen, to keep the drift tube field free and to cut off the operating mode. To suppress the TE_{11} mode, the drift tube is heavily loaded with dielectric rings and the length of the drift tube is extended.

2.3. Design of Beam Wave Interaction Structure

In high power amplifiers, when the device interaction length crosses the shortest critical length or SOL, device become unstable. The instabilities at the output interaction section are restrained by lowering its length to the start oscillation length (SOL), estimated through the analysis of backward wave oscillations (BWOs). To

ensure the stable operation of the multi-cavity gyro-twystron, an ideal operating point is optimized through the dispersion curve. Also, the bandwidth of the gyro-twystron is proportional to the slope of the cyclotron resonance line, defined as dispersion curve. Therefore the interaction circuit length is optimized so that the dispersion curve of the TE_{01} mode is tangent to the electron beam's cyclotron resonance line over a wide frequency range.

2.3.1. Dispersion Diagram and Backward Wave Analysis

The oscillation causes instability in the amplifier due to either an external or internal feedback process. Reflections at both ends of the interaction region provide external feedback. When the amplitude of the reflected signal crosses a threshold level, the wave amplification processes become regenerative, resulting in oscillation [126]. In high power amplifiers, when the device interaction length crosses the shortest critical length, device become unstable. So, the instabilities at the output interaction section are restrained by lowering its length to the start oscillation length (SOL), estimated through the analysis of backward wave oscillations (BWOs). To ensure the stable operation of the multi-cavity gyro-twystron, an ideal operating point is optimized through the dispersion curve.

The dispersion curve, which use to investigate the different instabilities occur in gyro amplifier. The dispersion curve shown in Figure 2.1, is derived from the waveguide mode line equation and beam mode line equation, as mentioned in eqn. 2.3

$$\left(\omega^2 - k_{\|}^2 c^2 - \omega_{cut}^2\right)\left(\omega - k_{\|} v_{\|} - \frac{s\omega_c}{\gamma_0} = 0\right)^2 = \frac{-4 I_b \beta_{\perp}^2 c^4 N\left(k_{mn}^2 B_{sm}\right)}{I_A \gamma_0 r_w^2 S_{mn}} \qquad [2.3]$$

Where N is the beam density parameter, $S_{mn} = \left(J_m^2 / X_{mn}^2\right)\left(X_{mn}^2 - m^2\right)$ and $B_{sm} = \left(J_{s\pm m}\left(k_{\perp} r_g\right)\right)\left(J_n^{'} k_{\perp} r_l\right)$, and I_A is Alfven current, r_g and r_l are the guiding center

radius and Larmor radius, respectively. The dispersion relation, in general, shows two types of instability that can occur in a gyro-TWT amplifier: absolute instability and convective instability. If the coupling between the cyclotron beam mode line and the waveguide mode line occurs in the positive $k_{\|}$ or k_z region, the wave propagates in the forward region, resulting in convective instability (TE_{01} mode). When this beam wave coupling occurs in the negative $k_{\|}$ or k_z region, the wave starts to grow in backward direction and causes backward wave oscillation, resulting in absolute instability (TE_{11}, TE_{02}, TE_{21}).

When the dispersion relation is solved the threshold limit of current (SOC) and waveguide length (SOL) for the onset of the absolute instability can be determined [126] as:

$$L_w = \left\{ \frac{4\gamma_0 k_{\|} I_A \beta_{\|}^3 J_m^2\left(x_{mn}\right)\left(x_{mn}^2 - m^2\right)}{k_{\perp}^4 I \beta_{\perp}^2 \left(J_n\left(k_{\perp} r_l\right)\left(J_{m\pm s}\left(k_{\perp} r_g\right)\right)\right)^2} \right\}^{1/3} \qquad [2.4]$$

The interaction length of the present gyro-twystron is optimized according to the eqn. 2.4, for the beam parameter of 65 kV, 6 A and operating mode and frequency is TE_{01} and 94 GHz, respectively. As shown in Fig 2.2.(a) the waveguide length is fixed at 12

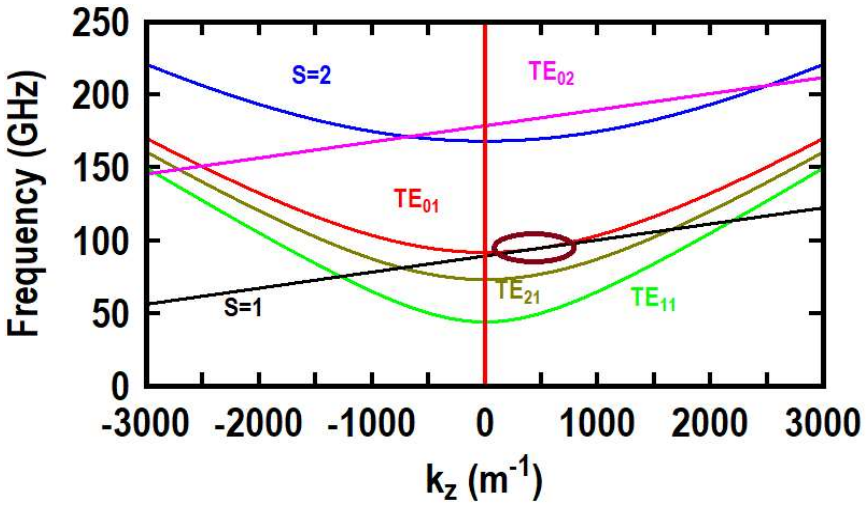

Figure 2. 1. Dispersion diagram of stagger tuned gyro-twystron

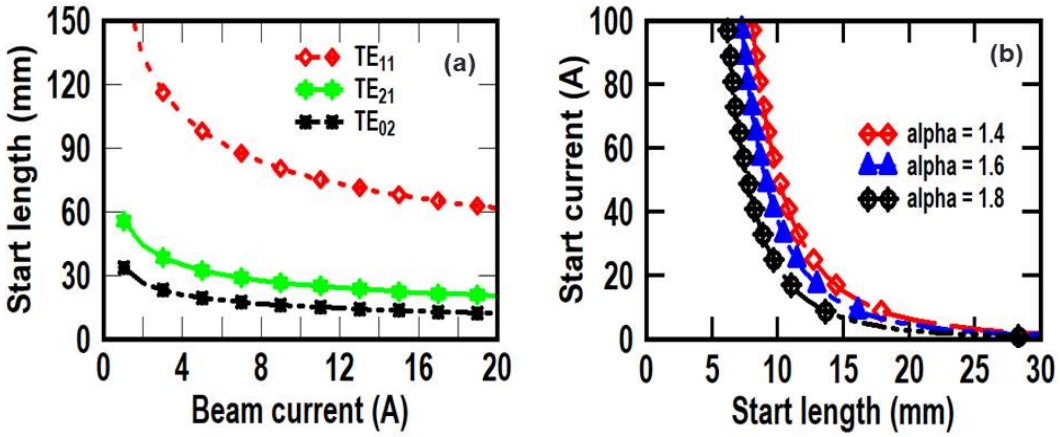

Figure 2. 2. (a) Start length versus beam current of each for different oscillating modes and (b) Start current versus start length at different pitch factor or alpha.

mm, well below the SOL of ~ 20 mm of the competing TE02 mode to limit the spurious oscillation. The start oscillation current of gyro-twystron is strongly depends on to the pitch factor (α), as it increases the transverse moment of electrons, which in turn reduces SOC [126]. A careful increment in pitch factor is required to enhance the kinetic energy of the electron, resulting in more amplification of the RF signal. Figure 2.2. (b). shows the change in SOC, corresponding to the SOL for the different pitch factor and observe an increment in SOC, with the pitch factor, enhance the beam wave synchronism and resulting in an increment in RF output power.

To achieve the maximum performance, an effective beam wave coupling is required [23], which is defined as coupling coefficient (C_i)

$$C_i = \frac{J_{m\pm s}^2\left(k_\perp r_b\right)}{J_m^2\left(x_{mn}\right)\left(x_{mn}^2 - m^2\right)} \qquad [2.5]$$

is depends on the gyrating beam positioning and transverse electric field. From the coupling coefficient expression, we can find the optimum electron beam launching position to have maximum coupling for the chosen mode. For the maximum coupling the beam radius and the guiding center radius is chosen as it gives the best beam wave coupling as well as it avoids the interception with the structure wall especially in drift

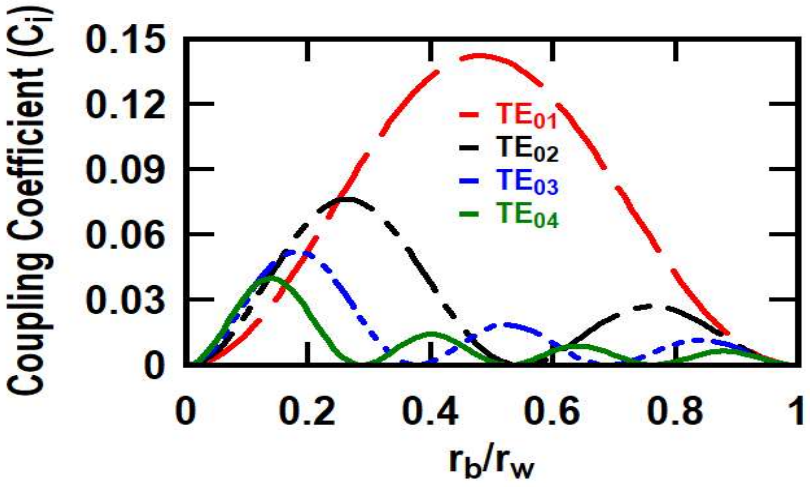

Figure 2. 3. Coupling coefficient of TE modes over beam position

tubes, which are having smaller radius. The normalized coupling coefficient with respect to the normalized beam radius (r_b/r_w) for the different modes is shown in Figure 2.3, and it is observed that the operating TE_{01} mode has the maximum coupling, limited to the beam radius of 0.45 times r_w to avoid the collision of electrons with the waveguide wall.

2.4. Basic Formulism of Stagger Tuned Gyro-Twystron

Nonlinear theory [12] is used to investigate the beam-wave interaction behaviour of relativistic gyro-twystron. At the input cavity, the relativistic gyrating electrons are described with the variable phase, which is influenced by an external DC magnetic field. The change in normalized energy (ψ), momentum (p) and phase (θ) over the normalized axial length (ξ), which are affected by the synchronism between the beam and RF input signal as [101]

$$\frac{d\psi}{d\xi} = \frac{p^{s_n}}{p_{\|}} \mathrm{Re}(F_n f^{'} e^{-j\theta}) \qquad [2.6]$$

$$\frac{dp_{\|}}{d\xi} = \frac{p_{\perp}^{s_n}}{p_{\|}} \mathrm{Re}(jF_n \frac{df^{'}}{d\xi} e^{-j\theta}) \qquad [2.7]$$

$$\frac{d\theta}{d\xi} + \frac{\gamma - s_n\Omega_0}{p_{\|}} = -s_n\gamma \frac{p_{\perp}^{s_n-2}}{p_{\|}} \mathrm{Re}[\mathrm{jF_n}\, f^{'} e^{-j\theta}(f^{'} - j\frac{p_{\|}}{\gamma}\frac{df^{'}}{d\xi})] \qquad [2.8]$$

where, s_n is the n[th] harmonic number, $p_{\|}$ and $p_{\perp}$ are the longitudinal and transverse momenta, respectively, θ and ξ are the electron phase and normalized axial length, respectively, and Ω_0 is the non-relativistic cyclotron frequency. The function $f^{'}$ explains the axial field variation in the cavity and F_n is the normalized field amplitude. The bunched electrons are departed from the drift tube with the phase of $\theta_d = \theta_1 - \int_{L_c}^{L_d} \frac{\gamma_1 - s_1\Omega_0}{p_{\|}} d\xi$, where, θ_1, L_c and L_d are the electron phase at the input of drift tube, input cavity length and drift tube length, respectively. To ensure the stable operation of the multi-cavity gyro-twystron, an ideal operating point is illustrated through the dispersion curve (Figure 2.1).

Broad banding of gyro-twystron is essentially required to make it an efficient source for numerous applications where wide bandwidth is needed. This can be achieved by tuning all cavities of gyro-twystron at different frequencies, i.e., stagger-tuning technique. The possibilities of stagger tuning have explored and extended the existing nonlinear theory for stagger-tuning analysis [119], [120]. An amplified signal with amplitude *Fn* and phase *(θ)* is expressed as

$$\frac{dF_n}{d\xi} = -I_0\left(1/2\pi\right) \int_0^{2\pi} \frac{(1-w)^{s/2}}{(1-bw)} e^{j\theta} d\theta \qquad [2.9]$$

$$\frac{d\theta}{d\xi} = \frac{1}{(1-bw)} \left\{ w - \nabla + s(1-w)^{((s-2)/2)}\, \mathrm{Img}(F_n e^{-j\theta}) \right\} \qquad [2.10]$$

where, $w=[2(1-\beta_{\|})(\gamma_0-\gamma)/\beta_{\perp}^2.\gamma_0]$, θ_2 and ∇ are the normalized energy, phase of gyrating electrons and normalized frequency mismatch, respectively, the parameter b is defined as the change in axial velocity of the electron beam, and $\beta_{\perp}$ and $\beta_{\|}$ are normalized transverse and axial velocities, respectively. The efficiency of beam-wave interaction is defined as, $\eta=\beta_{\perp}^2\eta_{\perp}/2(1-h\beta_{\|})[(\gamma_0-1)/\gamma_0]$, where, $\eta_{\perp}$ is the orbital efficiency that gives the change in electron orbital momentum and *h* is normalized axial wave number. For a multi-section gyro-amplifier, the field amplitude is defined as,

$$|F_m|^2=\frac{4I_0^2|u_m|^2|\mathrm{H}_m|^2}{(I_0\chi_m^{''}-1)^2+(\delta_m+I_0\chi_m^{'})^2} \qquad [2.11]$$

The phase of the resonating field is defined as,

$$\tan\psi_m=\left(\delta_m+I_0\chi_m^{'}\right)/\left(1-I_0\chi_m^{''}\right) \qquad [2.12]$$

where, u_m is the transit effect in cavities, $\chi_m^{'}$ and $\chi_m^{''}$ are the real and imaginary parts of susceptibility, respectively, I_0 and A_s are normalized current and field intensity, respectively, H_m is the phase bunching effect in the drift tube region, δ_m is the frequency detuning between the device operating frequency and m^{th} cavity resonating frequency, which is defined as, $\delta_m=2Q_m(f-f_m)/f$, where, *f* is the operating frequency and f_m and Q_m are resonating frequency and quality factor of m^{th} cavity, respectively. If the pre-bunching cavities are following "point-gap" model, *i.e.* cavities are short enough, then the field amplitude and phase of the resonating field are written as,

$$|F_m|^2=\left(4I_0^{'2}|H_m|^2\right)/\left(1+\delta_m^{'2}\right) \qquad [2.13]$$

$$\tan\psi_m=\delta_m^{'} \qquad [2.14]$$

where, $\delta_m^{'}=\delta_m/(1+I_0)$ and $I_0^{'}=I_0/(1+I_0)$. For m^{th} pre-bunching cavities,

$$\frac{|F_o|^2}{|F_m|^2}\frac{|F_m|^2}{|F_{m-1}|^2}\frac{|F_{m-1}|^2}{|F_{m-2}|^2}....\frac{|F_1|^2}{|A_s|^2} \qquad [2.15]$$

These combined equations allow us to analyze the effect of the stagger tunning on the overall gain, bandwidth and gain bandwidth product of the stagger tuned gyro-twystron.

The gain of multicavity gyro-twystron depends on the field excited inside the cavities, which is expressed as, $A_s = 2\left(I_c P_d Q_{in}/P_{0\perp} Q_e\right)^{1/2}$. Here P_d, Q_{in} and Q_e are the drive power, input cavity's quality factor and external quality factor. The beam power $P_{0\perp}$ is depends on the applied beam voltage and beam current. The over all gain of the stagger tuned gyro-twystron is expressed as

$$G = 10\log\left(\frac{P_{o\perp}|F_o|^2}{P_{in}I_o(1-h\beta_{||})}\right) \qquad [2.16]$$

For studying the effect of stagger-tuning the gain for the stagger tuned gyro-twystron is defined as the summation of two term,

$$G = G_{\text{var}} + G_{\text{const}} \qquad [2.17]$$

where, G_{const} is the gain for synchronously tuned amplifier and G_{var} is the variable gain that describe the stagger tunning effect, and defined as

$$G_{\text{var}} = 10\log\left(|F_o|^2/|A_s|^2\right) \qquad [2.18]$$

where F_o is the field intensity at the output waveguide. The expressions for G_{var} and G_{const} normalized in such a way that when frequency mismatch in all the cavities become zero the variable gain term G_{const} vanishes. The cyclotron resonance mismatch or stagger tuning parameter ∇, that govern the change in variable gain at the output waveguide, is given by,

$$\nabla = 2(\omega_c - k_0 v_0 - s\Omega_0)/\left(\beta_\perp^2 \omega\right) \qquad [2.19]$$

Where k_0 and v_0 are axial propagation constant and the axial beam velocity

The 3-dB bandwidth in terms of the normalized frequency detuning parameter is related to conventional bandwidth as

$$BW_{\nabla} = (2/\beta_{\perp}^{2})BW \qquad [2.20]$$

The normalized gain-bandwidth product (Φ) is defined as the ratio of the gain-bandwidth product of the stagger tuned amplifier to the synchronously tuned amplifier, which is defined as

$$\Phi = BW_{\nabla} * G_{\nabla} / BW * G \qquad [2.21]$$

where, BW_{∇} and G_{∇} are the bandwidth and gain due to stagger tuning, respectively, and BW and G are the bandwidth and gain of the synchronously tuned amplifier, respectively.

2.5. Gain and Bandwidth Analysis of Stagger Tuned Gyro-Twystron

A multi-cavity gyro-twystron [121] driven by 65 kV, 6A with the beam velocity ratio ~1.6 is investigated to study its performance through its gain, bandwidth and gain-bandwidth product. When all the cavities resonate at the same frequency or are tuned synchronously, the gain is at its highest, or the loss of gain is at its lowest. As the tuning of the cavities changes, the gain goes down [Figure2.4]. This drop in gain is due to the change in the resonating frequencies of the cavities, resulting in a decrement in the overall peak amplitude compared to synchronously tuned, in which all cavities have the same resonating peak. From Figure2.4 it is observed that at the optimized stagger tuning parameter of 0.6, the gain degradation is ~ 3 dB and this analytical finding is validated against 3-D PIC simulation result and find a close agreement. In a stagger tuned amplifier, every individual cavity has its 3 dB bandwidth, and the overall effect produces a better wideband characteristic, in contrast, narrow band characteristic of a

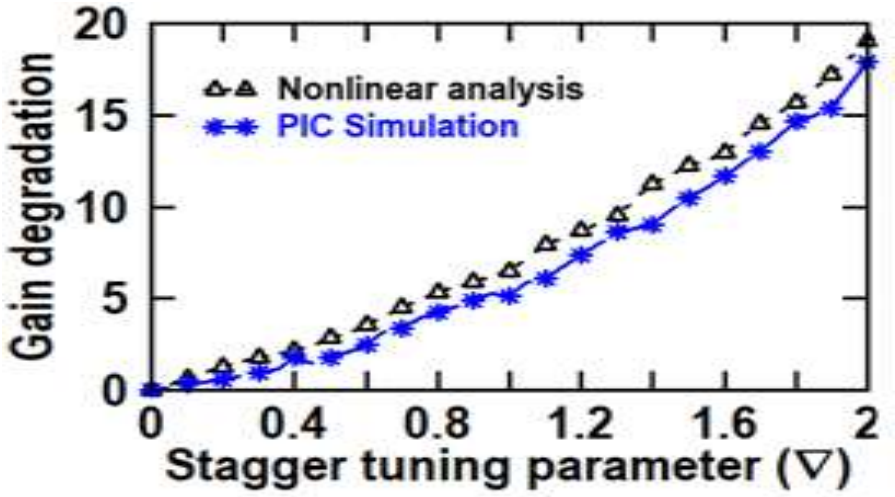

Figure 2. 4. Gain degradation with respect to the stagger tuning parameter

synchronous tuned amplifier. The stagger tuning of cavities [Figure 2.5] allows an enhancement in the normalized bandwidth at the cost of gain. At the optimized stagger tuning parameter of 0.6, the bandwidth is improved by ~2.5 times of the synchronously tuned cavities. It is observed that there is a trade-off between the bandwidth and the gain of the stagger tuned gyro-twystron. The cavities are stagger-tuned to significantly maintain the device's gain and improve the bandwidth substantially. The stagger tuning technique is used to achieve a maximum gain-bandwidth product, which is an important figure of merit of any microwave amplifier. Therefore, a trade off in the gain-bandwidth product of the gyro-twystron amplifier is needed for its performance evaluation rather than characterizing its performance simply by gain or bandwidth. Taking these facts into account, the normalized gain-bandwidth product of the designed three cavity stagger-tuned gyro-twystron amplifier is plotted against the stagger-tuning parameter in Figure2.6. The variation of the normalized gain-bandwidth product (GBW) of the device with the stagger tuning parameter ∇ found by nonlinear analysis has been validated against the PIC simulation, as illustrated in Figure 2.6.

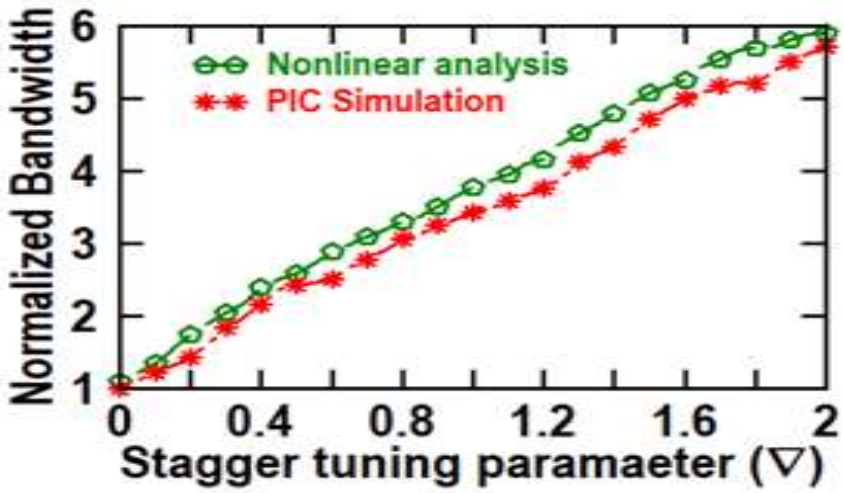

Figure 2. 5. Change in bandwidth with respect to the stagger tuning parameter

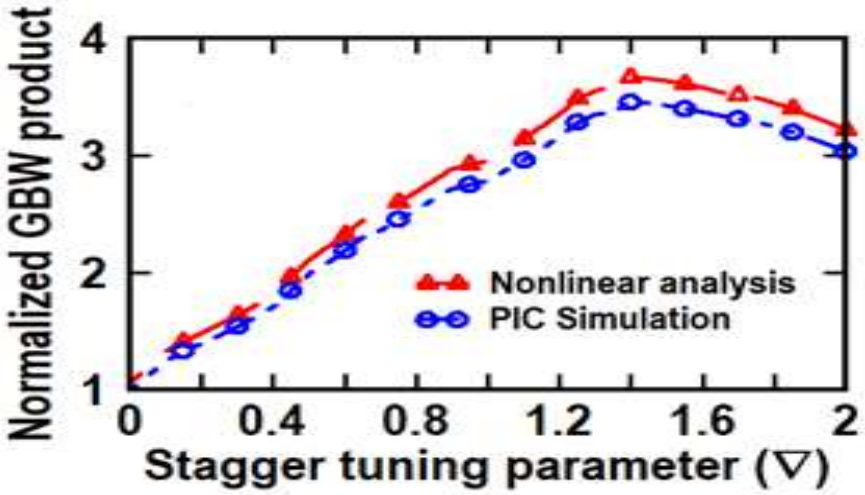

Figure 2. 6. Normalized gain bandwidth product as a function of stagger-tuning parameter.

It is also observed that the analytically obtained GBW of the device is reached the peak value for the same value of ∇ and closely agreed with its simulated value. The decrease in the value of GBW beyond a certain value of ∇ can be attributed to the strong gain degradation of the device, beyond that value.

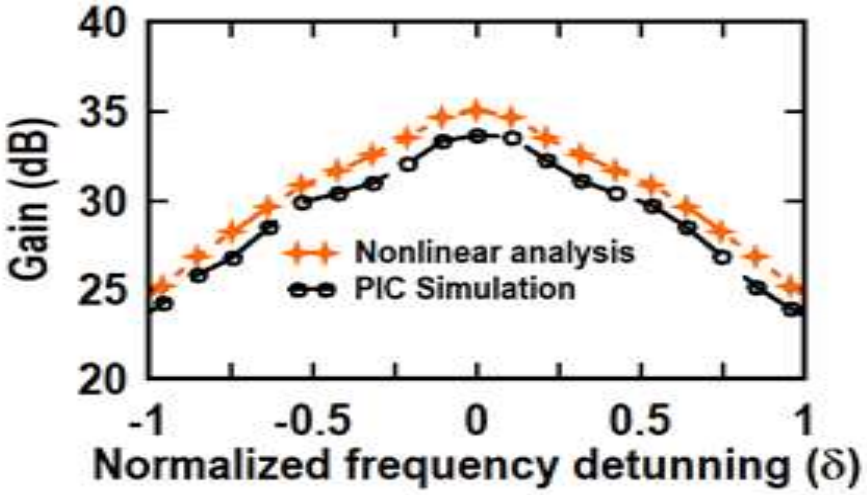

Figure 2. 7. Gain variation as a function of frequency detuning at the specific value of stagger tuning parameter.

The dependencies of gain upon the normalized frequency detuning (δ) is shown in Figure 2.7, for stagger-tuning parameter (∇) of 0.6. As observed from Figure 2.7, the gain variation is almost symmetric with respect to normalized frequency detuning (δ) of the RF cavities. It means that the same amount of gain degradation will occur on both sides of the curve for a particular value of stagger tuning, either ∇ is positive or negative [119]. The analytical observation of gain variation with respect to the normalized frequency detuning, is verified with the simulation observations and found that they are in close agreement. The variation of normalized GBW of the device for different gain of the synchronized cavities, with respect to the stagger tuning parameter is illustrated in Figure 2.8 (a). The value of ∇ at which the GBW of the device is reached an optimum value that remains the same for various typical value of device gain considered in the present study. The maximum normalized GBW is achieved at a lesser value of stagger tuning parameter due to less degradation in the device gain. A parametric observation [Figure2.8.b] is made for the gain variation with the normalized frequency detuning, corresponding to the different stagger tuning parameter (∇), that verifies the above discussion of gain decrement with the change in stagger tuning parameter (∇).

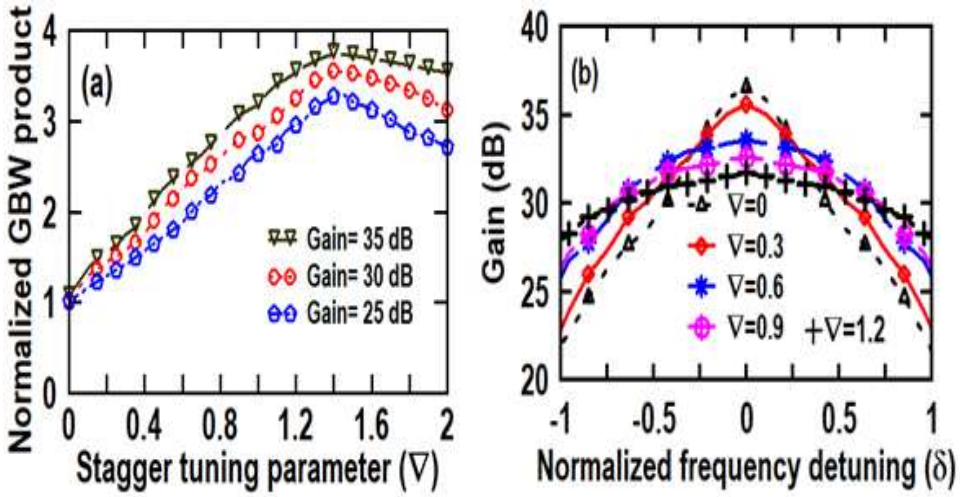

Figure 2. 8. (a) Normalized gain-bandwidth product Vs stagger tuning parameter and (b) gain Vs normalized frequency detuning.

If the value of delta is held constant and the number of cavities (N_c) is increased, the device gain will also increase; however, this will come at the expense of bandwidth, which can be compensated by the stagger tunning. Because of this improvement in the device gain, the normalized GBW product is now 1.4 times better when compared to the single cavity structure. This improvement is illustrated in Figure 2.9.

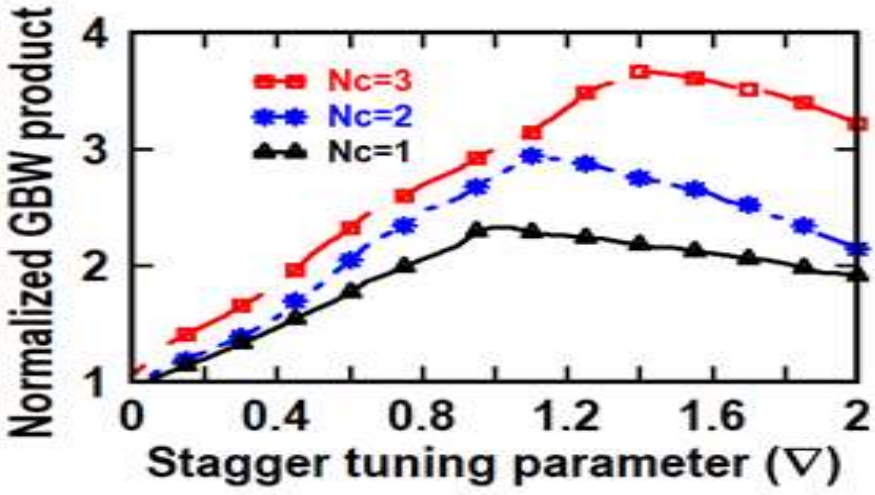

Figure 2. 9. Normalized GBW vs stagger tuning parameter for different number of cavities

In general, choosing a low - factor of the pre bunching cavity to increase bandwidth implies that a higher driver power is required to achieve efficient beam

bunching before the beam enters the output waveguide [121]. However, as the number of pre bunching cavities increases, the driver power required to achieve efficient bunching can become significantly lower. Figure 2.10 illustrates the variation of the normalized GBW product for various quality factor of the cavity, which shows that it affects the electron bunching and device gain. The normalized GBW product for the quality factor set Q_A ($\overline{Q}_1 = 1.2; \overline{Q}_2 = 1.05; \overline{Q}_3 = 1.25$) is observed as ~1.4 times as compared to quality factor set Q_B ($\overline{Q}_1 = 1.3; \overline{Q}_2 = 1.05; \overline{Q}_3 = 1.15$) and ~2 times over the quality factor set Q_C ($\overline{Q}_1 = 1.2; \overline{Q}_2 = 1.15; \overline{Q}_3 = 1.35$).

When the value of the stagger tuning parameter is increased to a higher level, there is an abrupt decrease in bandwidth after a certain limit, and this is due to the greater bunching effect [119]. This is due to the fact that the pre bunching of the beam now has a significantly greater effect on the gain curve, which results in a greater deviation in the gain curve. However, when the stagger tuning parameter is reduced to a lower value, these deviations are still within an acceptable range of variation.

The length of the waveguide is chosen wisely so as to keep the device gain and bandwidth at the desired level. If the waveguide length exceeds the SOL, the device will

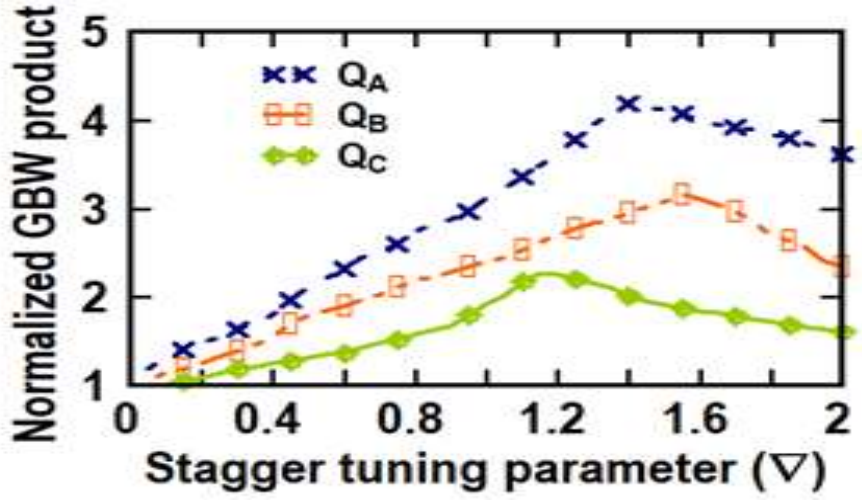

Figure 2. 10. Normalized GBW Vs stagger tuning parameter for different normalized quality factor.

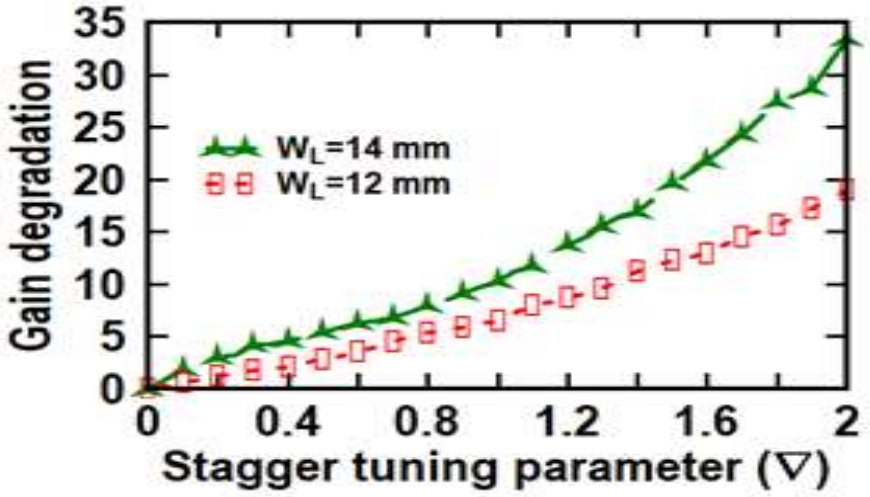

Figure 2. 11. Gain degradation Vs stagger tuning parameter for the fixed values of waveguide length.

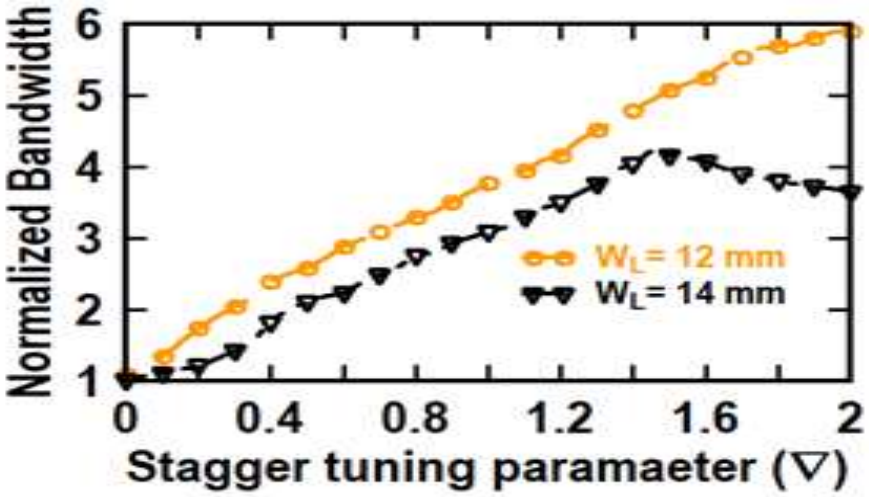

Figure 2. 12. Change in Bandwidth with the stagger tuning parameter for the different values of waveguide length.

start to oscillate; consequently, with the TE_{01} mode operating, other nearby competing modes will also be excited and start to interact with the amplified gyrating beam, result a decrement in the device's overall gain. [Figure 2.11]. For efficient transfer of energy and sufficient bandwidth, the minimum interaction length, W_L is chosen as 12 mm in the present stagger tuned three cavity gyro-twystron design. Figure2.12 shows the variation of normalized bandwidth with respect to stagger tuning parameter for a fixed waveguide length. It is observed that the bandwidth of the device decreases with the length and

simultaneously the undesired oscillation will start in the interaction region, if the length of the waveguide exceeds the SOL. Therefore, the length of the waveguide section is optimized for an optimal gain-bandwidth product.

2.6. Conclusion

In Chapter 2, the staggered three-cavity gyro-twystron amplifier is examined in greater detail in an attempt to identify ways to improve the amplifier's performance in terms of the device's bandwidth. One of the major requirements for a millimeter wave radar application is a wide bandwidth gyro amplifier. The current gyro-twystron, which employs three resonant cavities, can potentially utilise the stagger tuning method for bandwidth enhancement. The concept of stagger-tuning is frequently used in cavity-based devices, like conventional klystrons and gyro klystrons, to enhance their bandwidth. In this method, the different cavities resonate at slightly different frequencies, resulting in an increase in the device's bandwidth at the expense of its gain. The same concept is used in this chapter to improve the bandwidth of the gyro-twystron amplifier, because the gyro-twystron is simply a combination of the input cavity section and the output waveguide section. This chapter develops a methodology for designing gyro-twystron amplifiers and analyses in depth how the stagger tuning technique has the potential to enlarge the bandwidth of the resulting devices. Each part of a gyro-twystron amplifier—the cavity, the drift tube, and the waveguide has its own set of design challenges, and these are all explored in the present chapter. In addition, we have investigated a trade off between gain and bandwidth, as well as a gain-bandwidth product, with regard to the stagger tuned gyro-twystron. The gain-bandwidth product of an amplifier is an essential factor that is frequently used as a measure of the device's performance. The numerically developed formalism is used to study the effect of stagger tuning on the various factors of the gyro-twystron, and this analytical finding has been

confirmed with the 2-D PIC simulation results and found an acceptable agreement between the results. The overall finding of this chapter is as discussed below:

- The operating principle and the fundamental concept related to beam wave interaction has presented to understand the amplification in gyro-twystron.
- The theories related to the stagger tunning technique developed by various researchers has extend to analysed the performance of the stgger tuned gyro-twystron.
- Parametric observation has done related to stagger tunning , and observe significant enhancement in bandwidth .
- The analytical finding related to stagger tunning has implemented in CST environment and find a closed agreement.